trodes located at the left and right black dots, respectively, on the top portion of Fig. 2G.

An alternative interpretation of the data is that a circular wave of activity propagates radially from an origin at the initial site of activation. Our data are not compatible with this notion. There was a lack of burst activity in TRNs located farther from the fixation zone than the initially active zone. For example, cell Q37 did not burst (Fig. 1E) after the start of 10° to 15° gaze shifts that began at the SC site of Q24.

Our observations suggest that a topographically represented motor command is transformed into the temporal firing pattern that motoneurons send to muscles (the so-called spatial temporal transform) when gaze is controlled throughout the spatial trajectory of neural activity on the motor map (*18*). This conclusion implies that traditional models of collicular control of gaze shifts need to be revised. In these models, the SC provides a command specifying only the initial vector of the intended gaze shift (*1*): a brainstem feedback control system is hypothesized to subtract actual gaze position from this signal, thereby yielding instantaneous gaze error, which drives the movement (*19*). Our results show that the SC itself spatially encodes the gaze error. Therefore, the SC may reside within the gaze feedback loop (*3, 8, 14*). This hypothesis is supported by observations that a sudden increase in the discharge frequency of TRN phasic bursts speeds up a gaze shift without affecting its accuracy (*8*). Such a finding is difficult to incorporate in traditional models of the SC, but, in a feedback control system wherein the SC provides the error signal, the higher velocities reduce gaze error more quickly, allowing shorter movement duration while maintaining accuracy.

REFERENCES AND NOTES

1. D. Guitton, in *Eye Movements*, R. H. S. Carpenter, Ed. (Macmillan, London, in press); D. L. Sparks, *Physiol. Rev.* **66**, 118 (1986); _____ and L. E. Mays, *Annu. Rev. Neurosci.* **13**, 309 (1990); R. H. Wurtz and J. E. Albano, *ibid.* **3**, 189 (1980).
2. A neuron in the superficial layers responds to visual stimuli restricted to a particular location in the contralateral half of the visual field. Neurons are arranged topographically to form a continuous representation (map) of this half-field (*1*).
3. D. Guitton, D. P. Munoz, H. L. Galiana, *J. Neurophysiol.* **64**, 509 (1990).
4. M. Crommelinck, M. Paré, D. Guitton, *Soc. Neurosci. Abstr.* **16**, 1082 (1990); D. Guitton, M. Crommelinck, A. Roucoux, *Exp. Brain Res.* **39**, 63 (1980); A. Roucoux, D. Guitton, M. Crommelinck, *ibid.*, p. 75.
5. A. Grantyn and R. Grantyn, *Exp. Brain Res.* **46**, 243 (1982); A. K. Moschovakis and A. B. Karabelas, *J. Comp. Neurol.* **239**, 276 (1985).
6. M. A. Meredith and B. E. Stein, *J. Neurophysiol.* **56**, 640 (1986).
7. D. P. Munoz and D. Guitton, *Brain Res.* **398**, 185 (1986).
8. D. P. Munoz, thesis, McGill University, Montreal (1988); _____ and D. Guitton, *Rev. Neurol. (Paris)* **145**, 567 (1989).
9. A. Berthoz, A. Grantyn, J. Droulez, *Neurosci. Lett.* **72**, 289 (1986); A. Grantyn and A. Berthoz, *Exp. Brain Res.* **57**, 417 (1985).
10. D. P. Munoz and D. Guitton, *Soc. Neurosci. Abstr.* **14**, 956 (1988); D. P. Munoz, D. M. Waitzman, R. H. Wurtz, *ibid.* **16**, 1084 (1990).
11. In six alert cats we studied the movement-related discharge characteristics of 16 antidromically identified TRNs. Of these, nine TRNs were recorded over a wide range of gaze-shift amplitudes, which provided the present database, whereas the other seven provided limited, but confirmatory, data. Methods have been described (*3, 8*). Cats were trained to generate orienting movements of different amplitudes and directions. An opaque barrier of variable width and orientation was positioned in front of the animal and a food target was presented on one side, then moved behind the barrier to remain hidden there. The trained animal oriented to the opposite side where it anticipated target reappearance. Thus, the animal oriented to a spatial locus devoid of a new sensory cue. Some experiments were designed [P. Pélisson, D. Guitton, D. P. Munoz, *Exp. Brain Res.* **78**, 654 (1989)] such that the animals oriented to the opposite side of the barrier in complete darkness. Similar results were obtained. To evaluate a neural discharge, it is usual to sum many responses into histograms, which give an estimate of the probability of an action potential occurring in each bin. To provide this estimate for single trials, we substituted Gaussian distributions, 20 ms wide, for each spike, thereby creating a spike probability density function (*14*). With this technique, the time of occurrence of a peak discharge was rarely ambiguous, but, when it was, the time of the earliest peak was plotted. The sum of such transformed rasters is the average spike density function.
12. More anterior positions on the motor map code smaller gaze shifts. The stereotactic position of Q24 was about 1.5 mm anterior to that of Q37. Microstimulation at the sites of Q24 and Q37 elicited 13° and 70° gaze shifts, respectively, which are close to the values predicted from Fig. 2.
13. The large range of gaze-shift amplitudes, over which the discharge of Q37 preceded movement onset, is characteristic of cells in the caudal SC and is due to the nonlinear characteristics of the motor map. In the caudal SC, a small zone of the motor map codes a wide range of amplitudes. Cell Q37 initiated ~60° gaze shifts. Extending the properties of cell Q24 to Q37 implies that the latter should discharge after the onset of gaze shifts larger than 60°. Given the compressed scaling of the posterior SC, 100° gaze shifts would probably have to be studied to discern this effect. Unfortunately, we could not test Q37 for amplitudes greater than 70° because our cats rarely generated such large single-step gaze shifts.
14. D. M. Waitzman, T. P. Ma, L. M. Optican, R. H. Wurtz, *ibid.* **72**, 649 (1988).
15. D. P. Munoz, D. Pélisson, D. Guitton, unpublished data.
16. In monkey, neurons that burst before saccades have finite movement fields: upper and lower limits in the direction and amplitude ranges over which the cell is active. By comparison, cat TRNs, such as cell Q24, had a lower limit on amplitude but no upper limit: they discharged for all amplitudes above the lower limit.
17. The limited range of eye motion (±25°) (*1, 3, 4*) in the cat prevented us from ascertaining whether or not these mechanisms operate to drive saccades in the cat whose head is held fixed.
18. Theoretical considerations related to and predicting moving activity patterns on the motor map of the SC were proposed by W. Pitts and W. S. McCulloch [*Bull. Math. Biophys.* **9**, 127 (1947)]. Additional analyses have been conducted by J. Droulez and A. Berthoz [in *Neural Computers*, R. Eckmiller and C. v. d. Malsburg, Eds. (Springer-Verlag, Berlin, 1988), pp. 345–358; *Proc. Natl. Acad. Sci. U.S.A.*, in press], and P. Lefebvre and H. L. Galiana [*Soc. Neurosci. Abstr.* **16**, 1084 (1990)].
19. J. H. Fuller, H. Maldonado, J. Schlag, *Brain Res.* **271**, 241 (1983); D. Guitton, R. M. Douglas, M. Volle, *J. Neurophysiol.* **52**, 1030 (1984); D. Guitton and M. Volle, *ibid.* **58**, 427 (1987); V. P. Laurutis and D. A. Robinson, *J. Physiol. (London)* **373**, 209 (1986); D. Pélisson and C. Prablanc, *Brain Res.* **380**, 397 (1986); _____, C. Urquizar, *J. Neurophysiol.* **59**, 997 (1988); R. D. Tomlinson and P. S. Bahra, *ibid.* **56**, 1558 (1986).

20. Supported by the Medical Research Council of Canada, the Fonds de la Recherche en Santé du Québec, and a stipend from the Montreal Neurological Institute (D.P.M.).

10 August 1990; accepted 7 December 1990

Second Structural Motif for Recognition of DNA by Oligonucleotide-Directed Triple-Helix Formation

PETER A. BEAL AND PETER B. DERVAN*

Relative orientations of the DNA strands within a purine·purine·pyrimidine triple helix have been determined by affinity cleaving. A purine-rich oligonucleotide bound in the major groove of double-helical DNA antiparallel to the Watson-Crick purine strand. Binding depended upon the concentration of multivalent cations such as spermine or Mg^{2+}, and appeared to be relatively independent of pH. Two models with specific hydrogen-bonding patterns for base triplets (G·GC, A·AT, and T·AT) are proposed to explain the sequence specificity of binding. The two models differ in the conformation about the glycosyl bond (syn or anti) and the location of the phosphate-deoxyribose backbone in the major groove of DNA. This motif broadens the structural frameworks available as a basis for the design of sequence-specific DNA binding molecules.

PYRIMIDINE OLIGONUCLEOTIDES BIND specifically to purine sequences in double-helical DNA to form a local triple-helical structure (*1–4*). These oligonucleotides bind in the major groove parallel to the Watson-Crick (W-C) purine strand through the formation of Hoogsteen hydrogen bonds. Specificity is derived from thymine (T) recognition of adenine-thymine base pairs (T·AT base triplets) and protonated cytosine (C+) recognition of guanine-cytosine base pairs (C+GC) base triplets). Less well under-

stood is a triple-helical motif in which a purine-rich oligonucleotide binds duplex DNA (*5–8*).

Mixtures of poly G and poly C form stable 2:1 complexes [poly(G·GC)], and preparations of poly(A), when mixed with poly(U), can form poly(A·AU) (*5, 6*). More recent studies of a poly(dG)·poly(dC) tract under torsional stress show that this sequence can support two distinct structures depending on the ionic conditions (*7*). Two triple helices were proposed, one with a pyrimidine strand folded back parallel to the purine strand of the W-C duplex (H-form) (C+GC triplets), and the other with a purine strand folded back antiparallel to the purine strand of the duplex (G·GC triplets) (*7*).

Evidence for a purine-rich oligonucleotide binding site-specifically to duplex DNA was provided when Hogan and co-workers demonstrated that a G-rich oligonucleotide represses transcription of the human c-*myc* gene in vitro (*8*). Although no hydrogen-bonding scheme was put forward, the binding of the purine-rich oligonucleotide was proposed to be based upon A·AT and G·GC triplets with the third purine-rich strand parallel to the purine strand of the W-C duplex (*8*). Our efforts to confirm this parallel purine-rich model failed (*2*). Moreover, we found that within a pyrimidine-rich oligonucleotide, G does not bind GC base pairs but rather, in some cases, binds TA base pairs (G·TA triplet) (*3*). This result suggested to us that there may be two different structural motifs for triple-helical recognition (*3*). We report the results of affinity-cleaving experiments that reveal the orientation of a purine-rich oligonucleotide bound in the major groove of double-helical DNA.

Models for possible base triplets formed when a purine-rich oligonucleotide binds duplex DNA (G·GC and A·AT) can be put forward based on structures previously proposed, logical hydrogen-bonding patterns, and a relatively fixed positioning of the phosphate-deoxyribose backbones (*6, 7, 9, 10*). In addition to possible G·GC and A·AT base triplets, one can consider a T·AT base triplet in which T in the third strand binds the AT base pair in a reverse-Hoogsteen manner (*11*).

We chose as our target binding site a 19-bp purine sequence, 5′-$AG_3AG_4AG_4AG_3A$-3′, within a 648-bp restriction fragment. The target sequence is identically read

Arnold and Mabel Beckman Laboratories of Chemical Synthesis, Division of Chemistry and Chemical Engineering, California Institute of Technology, Pasadena, CA 91125.

*To whom correspondence should be addressed.

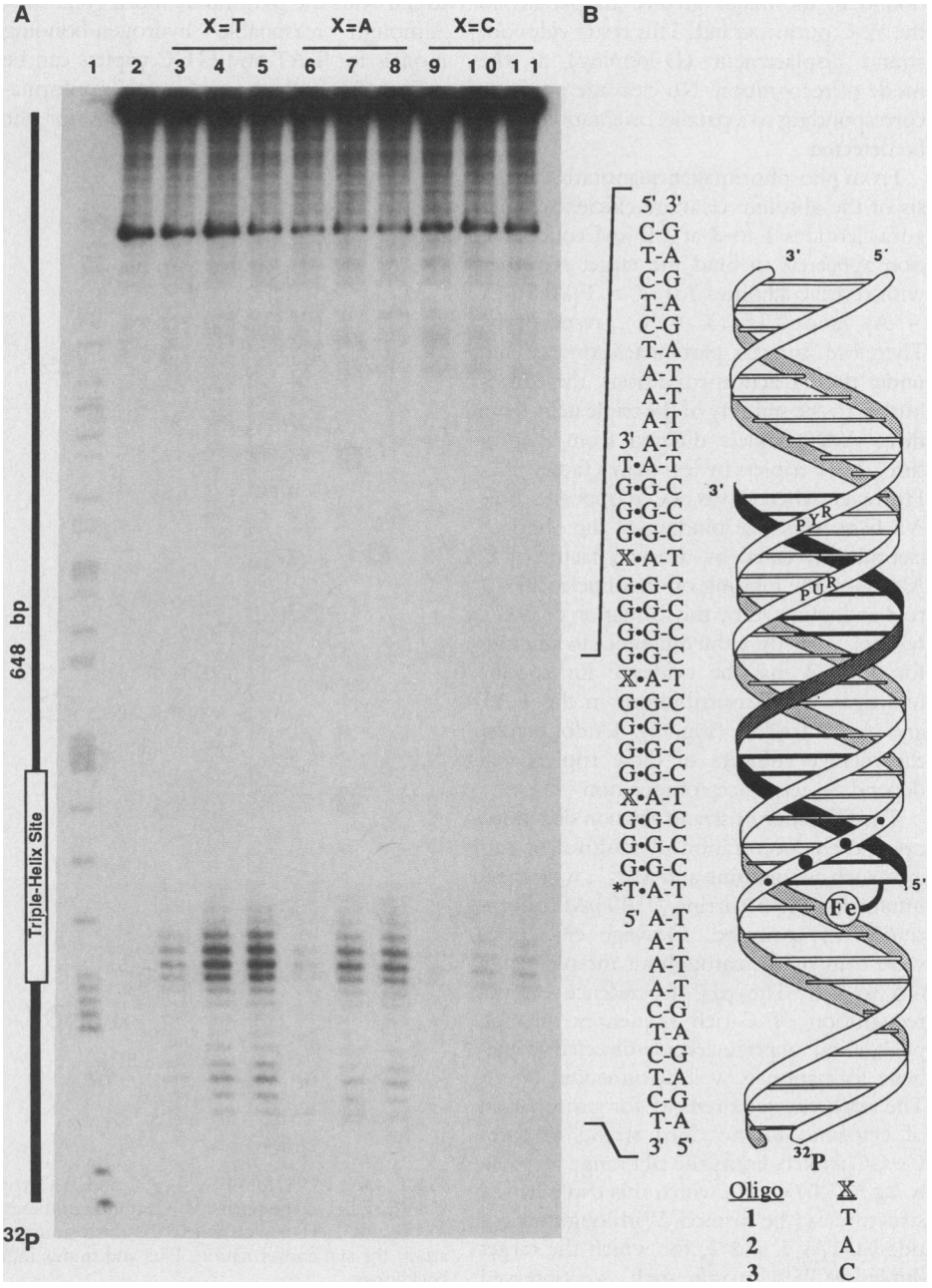

Fig. 1. (**A**) Autoradiogram of an 8% polyacrylamide sequencing gel showing the dependence of cleavage efficiency on sequence composition of oligonucleotides **1** to **3**, each at three different concentrations (0.1, 0.5, and 1.0 μM). The cleavage reactions were performed on the Hind III–Ssp I restriction fragment of plasmid pPBAG19 labeled at the 3′ end with ^{32}P (*15*). The reactions were carried out by combining a mixture of oligonucleotide-EDTA and 2.5 equivalents of $Fe(NH_4)_2(SO_4)_2{\cdot}6H_2O$ with the ^{32}P-labeled restriction fragment [~100 nM in base pairs, ~10,000 cpm] in a solution of tris acetate, pH = 7.8 (50 mM), NaCl (10 mM), spermine (100 μM), and calf thymus DNA (100 μM in base pairs), which was then incubated at 24°C for 1 hour. Cleavage reactions were initiated by the addition of dithiothreitol (DTT) (4 mM) and allowed to proceed for 12 hours at 24°C. The reactions were stopped by precipitation with ethanol, and the cleavage products were analyzed by gel electrophoresis. Lane 1, products of an A-specific cleavage reaction (*14*). Lane 2, control showing intact 3′ end-labeled restriction fragment obtained after treatment according to the cleavage reactions in the absence of oligonucleotide-EDTA·Fe. Lanes 3 to 11, cleavage products produced by oligonucleotides-EDTA·Fe of general sequence $T^*G_3XG_4XG_4XG_3T$-3′: lanes 3 to 5, X = T; lanes 6 to 8, X = A; and lanes 9 to 11, X = C. Concentrations of oligonucleotide-EDTA·Fe **1** to **3**: lanes 3, 6, and 9, **1** to **3** at 0.1 μM; lanes 4, 7, and 10, **1** to **3** at 0.5 μM; and lanes 5, 8, and 11, **1** to **3** at 1.0 μM. Cleavage efficiencies were quantitated by using storage phosphorimaging plates with a Molecular Dynamics 400S PhosphoImager. (**B**) Ribbon model and sequence of local triple-helical complex between oligonucleotides-EDTA·Fe **1** to **3** and the target sequence. Circles represent backbone positions of cleavage. Size of circles represent extent of cleavage. The third strand is located near the center of the major groove of the double-helical DNA based upon models in Fig. 2A.

from 3′ to 5′ or 5′ to 3′. Therefore, it could a priori support two putative triple-helical structures within a purine·purine·pyrimidine motif with the third strand parallel or antiparallel to the W-C purine strand. Oligonucleotides **1** to **3** of sequence composition 5′-T*$G_3XG_4XG_4XG_3$T-3′ (where X = T,A,C, respectively) were synthesized with thymidine-EDTA (T*) at each 5′ end (*12*). Oligonucleotides-EDTA·Fe **1** to **3** (0.1 to 1.0 μM, pH 7.8, 24°C) cleaved the double-helical DNA at the target site but with different efficiencies (Fig. 1). Cleavage occurred near the 3′ end of the purine tract. The cleavage maximum on each strand was shifted asymmetrically in the 5′ direction. The asymmetry and location of the cleavage pattern on one end of the binding site indicate that oligonucleotides **1** to **3** were bound in the major groove antiparallel to the W-C purine strand. This result rules out strand displacement (D-looping) as the mode of recognition. No cleavage products corresponding to a parallel orientation could be detected.

From phosphorimager quantitative analysis of the absolute cleavage efficiencies, oligonucleotides **1** to **3** at 1.0 μM concentration appeared to bind the target sequence with relative affinities 1.0 (X = T), 0.56 (X = A), and 0.16 (X = C), respectively. Therefore, for this particular sequence and under these reaction conditions, the contribution to the stability of the triple helix from three A·AT triplets differed from that of three T·AT triplets by less than a factor of 2. However, when C was placed opposite three AT base pairs, the binding of the oligonucleotide decreased by nearly a factor of 8. Although the binding of oligonucleotides **1** to **3** is dominated by the formation of G·GC triplets, we believe the difference in affinities for **1** to **3** may be evidence for specific hydrogen bond contributions in the T·AT and A·AT triplets (Fig. 2). Undoubtedly, the relative affinities of these triplets will depend on sequence composition (*13*).

The efficiency of strand scission depended upon the concentration of multivalent cations such as spermine and Mg^{2+}, with maximum cleavage occurring ≥100 μM concentration of spermine. Cleavage efficiencies were comparable throughout the pH range 6.6 to 7.8. The pH dependence on the recognition of G-rich sequences through pyrimidine oligonucleotide-directed triple-helix formation is well documented (*1–4*). The apparent requirement for protonation of cytosines in the third strand to form C+GC triplets limits the pH range (typically ≤pH 7.0) within which this triple-helical structure can be formed. With oligonucleotide-EDTAs **1** and **2**, for which the target duplex is 75% guanine-rich, we observed efficient cleavage at pH 7.8. Therefore, purine-rich oligonucleotides bound double-helical DNA in a relatively pH-independent fashion.

Within the constraints of our experimental data that the third strand is antiparallel to the purine-rich W-C strand, models of possible hydrogen-bonding patterns for A·AT, T·AT, and G·GC base triplets place the phosphate-deoxyribose backbone in different locations in the major groove depending on whether the base in the third strand is in the anti or syn conformation (Fig. 2). The anti conformation would generate a structure with the phosphate-deoxyribose backbone centrally located in the major groove of the double helix (Fig. 2A). The syn conformation would place the backbone in a similar location in the major groove as found with the pyrimidine motif (Fig. 2B). Although reasonable hydrogen-bonding models for T·AT and G·GC triplets can be written for both the syn or anti conformations of the third strand, models for the A·AT triplet suggest the most reasonable structure is the anti conformation (Fig. 2A). Hence, we tentatively favor the anti conformation and placement of the phosphate-deoxyribose backbone near the center of the major groove located more equidistant between the W-C strands (Fig. 2A). This triple-helix structure differs from the pyrimidine-rich motif in which the phosphate-deoxyribose backbone is located proximal (and parallel) to the purine W-C strand. Motif descriptions based on the terms "pyrimidine-rich" and "purine-rich" will become less meaningful as mixed sequence oligonucleotides are used. Similarly, parallel versus antiparallel motif (to the purine W-C strand) may not be precise as recognition of mixed purine-pyrimidine sequences of duplex DNA becomes possible. The contrast between the symmetric and asymmetric radial distribution of the backbones appears to be a useful distinguishing feature of the two triple-helical motifs.

Although there are apparently two differ-

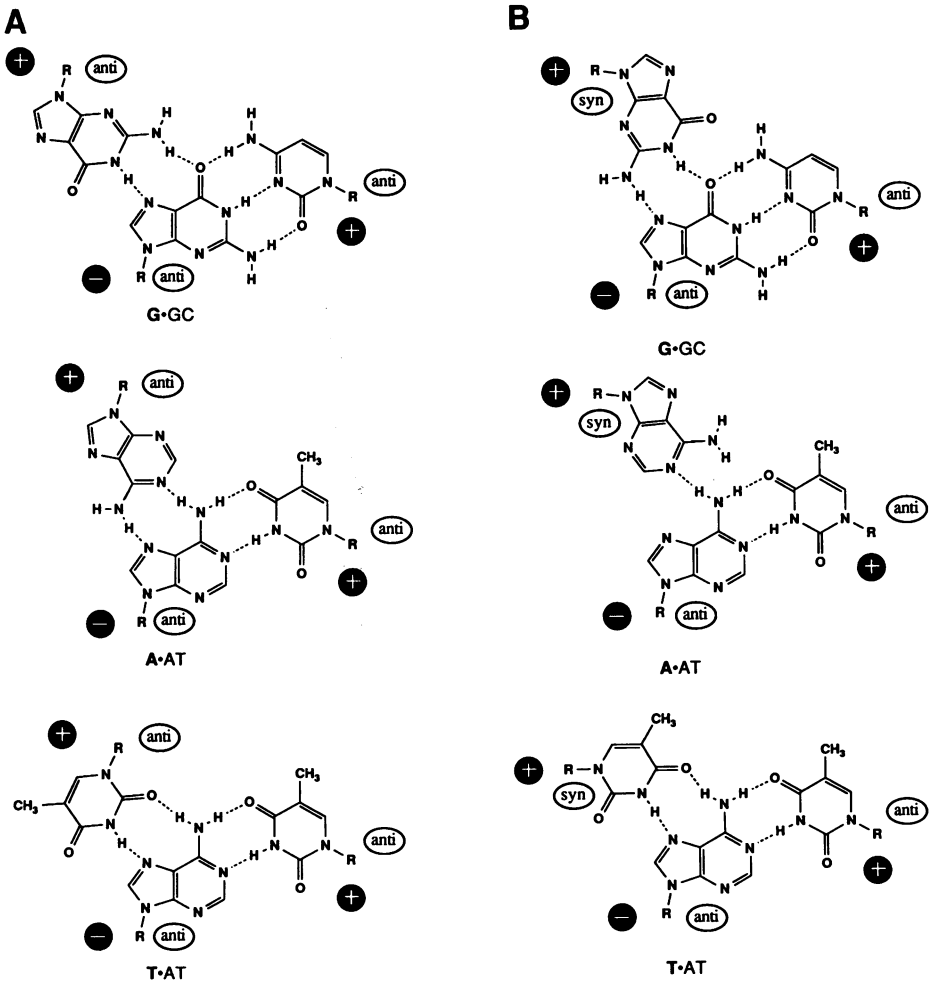

Fig. 2. (**A**) Models for G·GC, A·AT, and T·AT triplets within a triple-helix motif where the third strand is antiparallel to the purine W-C strand and bases are in the anti conformation. (**B**) Models for G·GC, A·AT, and T·AT triplets where the third strand is antiparallel to the purine W-C strand and the bases are in the syn conformation. Plus and minus indicate relative polarities of the phosphate-deoxyribose backbones.

ent structural classes of triple helices for oligonucleotide-directed recognition of double-helical DNA, both are currently limited to binding purine-rich tracts of DNA. Moreover, the sequence-composition dependence of the triplet stabilities within each triple-helix motif remains to be elucidated. High-resolution x-ray crystallographic data for either structural class does not yet exist.

REFERENCES AND NOTES

1. H. E. Moser and P. B. Dervan, *Science* **238**, 645 (1987); S. A. Strobel, H. E. Moser, P. B. Dervan, *J. Am. Chem. Soc.* **110**, 7927 (1988); T. J. Povsic and P. B. Dervan, *ibid.* **111**, 3059 (1989); S. A. Strobel and P. B. Dervan, *ibid.*, p. 7286; K. J. Luebke and P. B. Dervan, *ibid.*, p. 8733; D. A. Horne and P. B. Dervan, *ibid.* **112**, 2435 (1990); S. A. Strobel and P. B. Dervan, *Science* **249**, 73 (1990).
2. L. J. Maher III, B. Wold, P. B. Dervan, *Science* **245**, 725 (1989).
3. L. C. Griffin and P. B. Dervan, *ibid.*, p. 967. This G·TA triplet was flanked by T·AT triplets. The relative stabilities of these triplets could differ depending on flanking sequences.
4. T. Le Doan *et al.*, *Nucleic Acids Res.* **15**, 7749 (1987); D. Praseuth *et al.*, *Proc. Natl. Acad. Sci. U.S.A.* **85**, 1349 (1988); J. C. Francois, T. Saison-Behmoaras, M. Chassignol, N. T. Thuong, C. Helene, *J. Biol. Chem.* **264**, 5891 (1989); V. I. Lyamichev, S. M. Mirkin, M. D. Frank-Kamenetskii, C. R. Cantor, *Nucleic Acids Res.* **16**, 2165 (1988); J. C. Francois, T. Saison-Behmoaras, N. T. Thuong, C. Helene, *Biochemistry* **28**, 9617 (1989); J. S. Sun *et al.*, *Proc. Natl. Acad. Sci. U.S.A.* **86**, 9198 (1989); P. Rajogopal and J. Feigon, *Nature* **339**, 637 (1989).
5. M. N. Lipsett, *J. Biol. Chem.* **239**, 1256 (1964); C. Mark and D. Thiele, *Nucleic Acids Res.* **5**, 1017 (1978).
6. S. L. Broitman, D. D. Im, J. Y. Fresco, *Proc. Natl. Acad. Sci. U.S.A.* **85**, 3781 (1987); A. G. Letai, M. A. Palladino, E. Fromm, V. Rizzo, J. R. Fresco, *Biochemisty* **27**, 9108 (1988).
7. Y. Kohwi and T. Kohwi-Shigematsu, *Proc. Natl. Acad. Sci. U.S.A.* **85**, 3781 (1988).
8. M. Cooney, G. Czernuszewicz, E. H. Postel, S. J. Flint, M. E. Hogan, *Science* **241**, 456 (1988).
9. N. G. Williams, L. D. Williams, B. R. Shaw, *J. Am. Chem. Soc.* **111**, 7205 (1989).
10. For tertiary base-pair interactions found in yeast tRNA, see discussion in C. R. Cantor and P. R. Schimmel, *Biophysical Chemistry*, part 1, *The Conformation of Biological Macromolecules* (Freeman, San Francisco, 1980), pp. 192–195.
11. W. Saenger, *Principles of Nucleic Acid Structure* (Springer-Verlag, New York, 1984), pp. 119–126.
12. G. B. Dreyer and P. B. Dervan, *Proc. Natl. Acad. Sci. U.S.A.* **82**, 968 (1985).
13. P. B. Dervan, B. Wold, L. J. Maher, J. Hacia, unpublished observations.
14. B. L. Iverson and P. B. Dervan, *Nucleic Acids Res.* **15**, 7823 (1987).
15. The plasmid pPBAG19 was constructed by inserting the sequence $d(A_2T_2(CT)_3A_5G_3AG_4AG_4AG_3A_5(CT)_3)$ into the large Eco RI–Xba I restriction fragment of pUC19. Reactions were performed on the 3′ end-labeled Hind III–Ssp I restriction fragment.

16. We are grateful to NIH for generous grant support and to DOE for a predoctoral fellowship to P.A.B.

22 August 1990; accepted 4 January 1991

An in Vivo Model of Somatic Cell Gene Therapy for Human Severe Combined Immunodeficiency

GIULIANA FERRARI, SILVANO ROSSINI, RAFFAELLA GIAVAZZI, DANIELA MAGGIONI, NADIA NOBILI, MONICA SOLDATI, GRACE UNGERS, FULVIO MAVILIO, ELI GILBOA, CLAUDIO BORDIGNON*

Deficiency of adenosine deaminase (ADA) results in severe combined immunodeficiency (SCID), a candidate genetic disorder for somatic cell gene therapy. Peripheral blood lymphocytes from patients affected by ADA⁻ SCID were transduced with a retroviral vector for human ADA and injected into immunodeficient mice. Long-term survival of vector-transduced human cells was demonstrated in recipient animals. Expression of vector-derived ADA restored immune functions, as indicated by the presence in reconstituted animals of human immunoglobulin and antigen-specific T cells. Retroviral vector gene transfer, therefore, is necessary and sufficient for development of specific immune functions in vivo and has therapeutic potential to correct this lethal immunodeficiency.

GENE THERAPY ASSUMES THAT A DEfinitive cure for a genetic disease should be possible by directing treatment to the abnormal gene rather than to secondary effects of its products (*1*). The altered gene can be complemented by introducing the normal gene into the cell genome with an appropriate vector. Retroviral vectors can be used to introduce exogenous DNA sequences into hematopoietic progenitors and pluripotent stem cells. Gene transfer has been successful in vitro and in vivo in the mouse (*2, 3*) and with lower efficiency in cultured hematopoietic progenitors that were derived from dogs and primates (*4, 5*), including humans (*6, 7*).

Deficiency of the enzyme adenosine deaminase (ADA) results in a variant of severe combined immunodeficiency (SCID), a lethal disorder usually treated with allogeneic bone marrow transplantation (*8*). Retroviral vectors derived from the N2 prototype can efficiently transduce the human ADA gene into established lymphoid cell lines that had been derived from ADA⁻ SCID patients (*9*) and into hematopoietic progenitors in both short- and long-term culture, with expression of the newly introduced ADA enzyme occurring in cells of myeloid and lymphoid lineages (*7*). However, in neither system was direct evidence available that expression of ADA activity in ADA⁻ cells would restore specific immune functions. To address this issue, we reconstituted a number of immunodeficient BNX (homozygous *bg/nu/x*^{id}) mice (*10*) with human ADA⁻ peripheral blood lymphocytes (PBLs) transduced with a retroviral vector (DCA, double-copy ADA) that contained a human ADA mini-gene (*11*). We then analyzed human cell survival, ADA gene transfer and expression, and reconstitution of immune functions.

BNX mice were injected with DCA-in-

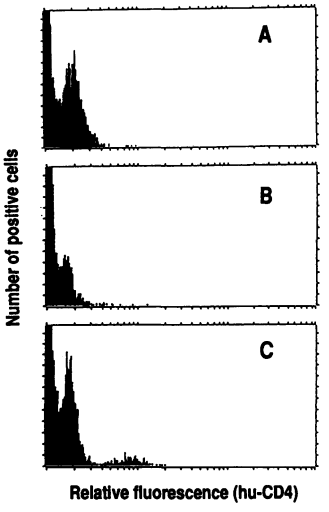

Fig. 1. Frequency of CD4⁺ human T cells in the spleen of recipient BNX mice 6 weeks after reconstitution. (**A**) Untreated animal. (**B**) Animal treated with mock-infected ADA⁻ PBLs. (**C**) Animal reconstituted with DCA-infected ADA⁻ PBLs (751). Animals 721, 751, 727, and 651 had frequencies of CD4⁺ human T cells varying between 2.1 and 4.2. All other animals had lower values. Fluorescein isothiocyanate (FITC)–conjugated MAbs to human (hu)-CD4 (T4), hu-CD8 (T8), hu-CD19 (B4), and hu-CD20 (B1) were obtained from Coulter Immunology (Hialeah, Florida). Isotype-matched MAbs were used for all analyses. Conjugated MAbs were chosen in order to reduce nonspecific binding. Furthermore, positive data were accepted only when background from negative controls (unstained cells from the experimental animal and stained cells from a mock-reconstituted animal) did not exceed 1% of positive cells. Flow analysis was done on a EPICS 751 cell sorter (Coulter Electronics, Hialeah, Florida), equipped with a 5 W Argon laser (Innova 90, Coherent Inc., Palo Alto, California).

G. Ferrari, S. Rossini, D. Maggioni, N. Nobili, M. Soldati, F. Mavilio, C. Bordignon, Laboratory of Hematology, Istituto Scientifico H.S. Raffaele, Milano, Italy. R. Giavazzi, Istituto di Ricerche Mario Negri Bergamo, Bergamo, Italy.
G. Ungers and E. Gilboa, Department of Molecular Biology, Memorial Sloan-Kettering Cancer Center, New York, NY, 10021.

*To whom correspondence should be addressed at Hematology Service, Istituto Scientifico H.S. Raffaele, via Olgettina, 60, 20132, Milano, Italy.

Second Structural Motif for Recognition of DNA by Oligonucleotide-Directed Triple-Helix Formation

Peter A. Beal and Peter B. Dervan

Science, **251** (4999), .
DOI: 10.1126/science.2003222